Transition from phase to generalized synchronization in time-delay systems

D. V. Senthilkumar,[1,a)] M. Lakshmanan,[1,b)] and J. Kurths[2,c)]

[1]*Centre for Nonlinear Dynamics, Department of Physics, Bharathidasan University, Tiruchirapalli-620 024, India*
[2]*Institute of Physics, University of Potsdam, Am Neuen Palais 10, 14469 Potsdam, Germany*

The notion of phase synchronization in time-delay systems, exhibiting highly non-phase-coherent attractors, has not been realized yet even though it has been well studied in chaotic dynamical systems without delay. We report the identification of phase synchronization in coupled nonidentical piecewise linear and in coupled Mackey–Glass time-delay systems with highly non-phase-coherent regimes. We show that there is a transition from nonsynchronized behavior to phase and then to generalized synchronization as a function of coupling strength. We have introduced a transformation to capture the phase of the non-phase-coherent attractors, which works equally well for both the time-delay systems. The instantaneous phases of the above coupled systems calculated from the transformed attractors satisfy both the phase and mean frequency locking conditions. These transitions are also characterized in terms of recurrence-based indices, namely generalized autocorrelation function $P(t)$, correlation of probability of recurrence, joint probability of recurrence, and similarity of probability of recurrence. We have quantified the different synchronization regimes in terms of these indices. The existence of phase synchronization is also characterized by typical transitions in the Lyapunov exponents of the coupled time-delay systems. © *2008 American Institute of Physics*. [DOI: 10.1063/1.2911541]

Synchronization of chaotic oscillations is one of the most fundamental phenomena exhibited by coupled chaotic oscillators. Since the identification of chaotic synchronization in identical systems, several different kinds of synchronizations such as generalized, phase, lag, anticipatory, and intermittent synchronizations have been identified and demonstrated. Among them, chaotic phase synchronization (CPS) plays a crucial role in understanding a large class of weakly interacting nonlinear dynamical systems. Even though the notion of CPS has been well studied in several low-dimensional chaotic dynamical systems during the past decade, CPS in time-delay systems (which are effectively infinite-dimensional) has not yet been identified and reported. A main problem here is to define even the notion of phase itself due to the presence of intrinsic multiple characteristic time scales of the chaotic attractors. Time-delay systems often exhibit complicated non-phase-coherent attractors (which do not have proper rotation around a fixed reference point) with many positive Lyapunov exponents. Hence, the conventional techniques available in the literature to define phase and to identify CPS cannot be used in the case of time-delay systems. In order to overcome this difficulty, we have introduced a nonlinear transformation which transforms the non-phase-coherent chaotic/hyperchaotic attractors of specific time-delay systems into phase-coherent attractors. The transformed attractors allow for the use of conventional methods to identify phase and CPS in time-delay systems. We have also confirmed the onset of phase and the transition from desynchronized state to phase synchronization and its subsequent transition to generalized synchronization as a function of coupling strength using recurrence-based indices. These results are also corroborated by the changes in the Lyapunov exponents of the coupled time-delay systems.

I. INTRODUCTION

Synchronization of chaotic oscillations is a fundamental nonlinear phenomenon observed in diverse areas of science and technology. Since the first identification of chaotic synchronization, several types of synchronization have been identified and demonstrated both theoretically and experimentally.[1–4] Complete (or identical) synchronization,[5–8] generalized synchronization,[9,10] and phase synchronization[11–13] are the three main types of synchronization that have been characterized by the difference in the degree of correlation between the interacting chaotic dynamical systems. Among these, chaotic phase synchronization (CPS) has become the focus of recent research as it plays a crucial role in understanding the behavior of a large class of weakly interacting dynamical systems in diverse natural systems including circadian rhythm, cardiorespiratory systems, neural oscillators, population dynamics, etc.[1,2,4] The definition of CPS is a direct extension of the classical definition of synchronization of periodic oscillations and can be referred to as entrainment between the phases of interact-

a)Electronic mail: skumar@cnld.bdu.ac.in.
b)Electronic mail: lakshman@cnld.bdu.ac.in.
c)Electronic mail: jkurths@gmx.de.

ing chaotic systems, while the amplitudes remain chaotic and, in general, noncorrelated[14] (see also Appendix A).

The notion of CPS has been investigated so far in oscillators driven by external periodic force,[15,16] chaotic oscillators with different natural frequencies and/or with parameter mismatches,[11,17–19] arrays of coupled chaotic oscillators,[14,20] and also in essentially different chaotic systems.[21,22] In addition, CPS has also been demonstrated experimentally in various systems, such as electrical circuits,[21,23–25] lasers,[26,27] fluids,[28] biological systems,[29,30] climatology,[31] etc. On the other hand, CPS in nonlinear time-delay systems, which form an important class of dynamical systems, has not yet been identified and addressed. A main problem here is to define even the notion of phase in time-delay systems due to the intrinsic multiple characteristic time scales in these systems. Studying CPS in such chaotic time-delay systems is of considerable importance in many fields, as in understanding the behavior of nerve cells (neuroscience), where memory effects play a prominent role, in physiological studies, in ecology, in lasers, etc.[1,2,4,32–36]

While studying CPS, one usually encounters the terminologies phase-coherent and non-phase-coherent chaotic attractors. If the flow of a dynamical system has a proper rotation around a fixed reference point, then the corresponding attractor is termed a phase-coherent attractor. In contrast, if the flow does not have a proper rotation around a fixed reference point, then the corresponding attractor is called a non-phase-coherent attractor. (More discussion on the distinction between phase-coherent and non-phase-coherent chaotic attractors along with an illustration is given below in Appendix A.) While methods have been well established in the literature to identify phase and to study CPS in phase-coherent chaotic attractors (see again Appendix A), methods to identify the phase of non-phase-coherent chaotic attractors have not yet been well established. Even the most promising approach based on the idea of curvature to calculate the phase of non-phase-coherent attractors is limited to low-dimensional systems, and unfortunately methods to identify phase and to study CPS in time-delay systems which often possess highly complicated hyperchaotic attractors have not yet been identified and reported.

Recently, we pointed out briefly the identification of CPS in unidirectionally coupled nonidentical time-delay systems exhibiting hyperchaos with highly non-phase-coherent attractors.[37] In this paper, we present our detailed results on the identification and existence of CPS in coupled piecewise-linear time-delay systems and in coupled Mackey–Glass time-delay systems with parameter mismatches. We will show the entrainment of phases of the coupled systems from an asynchronous state and its subsequent transition to generalized synchronization (GS) as a function of coupling strength. Phases of these time-delay systems are calculated using the Poincaré method after a newly introduced transformation of the corresponding attractors, which transforms the original non-phase-coherent attractors of both the systems into smeared limit-cycle-like attractors. Further, the existence of CPS and GS in both of the coupled systems is characterized by recently proposed methods based on recurrence quantification analysis and in terms of Lyapunov exponents

of the coupled time-delay systems. Thus, the main results of our paper are as follows:

(1) Suitable nonlinear transformation involving delay time can be introduced which transforms a chaotic/hyperchaotic non-phase-coherent attractor to a phase-coherent attractor. Then it is easier to find the onset of CPS, GS, etc. using these transformed phase-coherent attractors.
(2) Recurrence-based indices can be directly used to identify phase, CPS, and GS from the original non-phase-coherent chaotic/hyperchaotic attractors.
(3) Lyapunov exponents also work as a good guide for the synchronization transitions involving chaotic/hyperchaotic non-phase-coherent attractors.

The plan of the paper is as follows. In Sec. II, a brief discussion about the concept of CPS (the possibility of estimation of the phase in chaotic systems is presented in detail in Appendix A) and details of the time-delay systems, namely the piecewise linear time-delay system and the Mackey–Glass system under investigation, are presented. In Sec. III, we point out the existence of CPS and GS in unidirectionally coupled piecewise-linear time-delay systems using the Poincaré section technique (after the introduced transformation), recurrence quantification analysis, and Lyapunov exponents of the coupled systems. We will also discuss the existence of CPS and GS in unidirectionally coupled Mackey–Glass time-delay systems in Sec. IV, using the above three different approaches. Finally in Sec. V, we summarize our results.

II. CPS AND TIME-DELAY SYSTEMS

CPS has been studied extensively during the past decade in various nonlinear dynamical systems as discussed in the Introduction. However, only a few methods have been available in the literature[1,4] (for more details, see Appendix A) to calculate the phase of chaotic attractors, but unfortunately some of these measures are restricted to phase-coherent chaotic attractors, while the others to non-phase-coherent chaotic attractors of low-dimensional systems. It is to be noted that these conventional methods available so far in the literature (as discussed briefly in the Appendix A) to identify phase of the phase-coherent/non-phase-coherent attractors cannot be used in the case of time-delay systems in general, as such systems will very often exhibit more complicated attractors with more than one positive Lyapunov exponent. Correspondingly, methods to calculate the phase of non-phase-coherent hyperchaotic attractors of time-delay systems are not readily available. The most promising approach available in the literature to calculate the phase of non-phase-coherent attractors is based on the concept of curvature,[38] but this is often restricted to low-dimensional systems. However, we find that this procedure does not work in the case of nonlinear time-delay systems in general, where very often the attractor is non-phase-coherent and high-dimensional. Hence defining and estimating phase from the hyperchaotic attractors of the time-delay systems itself is a challenging

task, and so specialized techniques/tools have to be identified to introduce the notion of phase in such systems.

It is to be noted that a variety of other nonlinear techniques such as mutual information, recurrence analysis, predictability, etc. can be used to identify basic types of synchronization.[39] In particular, mutual information, predictability, and their variants have been used for characterizing the existence of complete synchronization, generalized synchronization, and the interdependencies among the measured time series of dynamical systems.[1,40–42] Mutual information can also be used to measure the degree of PS,[43] see also Sec. III A below, provided that phase is already defined. Recently, recurrence-based indices are shown to be excellent quantifiers[39] of basic kinds of synchronization including CPS in low-dimensional systems and even in the case of noisy, nonstationary data. However, as far as we know, predictability cannot be used either to define or to identify PS. In any case, these measures have not been used so far to identify phase or CPS in time-delay systems.

In order to define/estimate phase and CPS in time-delay systems, in this paper we have introduced three different approaches. First, we have introduced a nonlinear transformation involving time-delay variable that transforms the non-phase-coherent attractors into phase-coherent attractors. After this transformation of the original non-phase-coherent attractor, the transformed attractor allows one to use the conventional techniques. Next, we have used the recently introduced recurrence-based indices for the first time in time-delay systems to identify the onset of PS and subsequent transition to GS. Finally, the transition is also confirmed by the changes in the spectrum of Lyapunov exponents of the coupled time-delay system. Further, we find that all three approaches are in good agreement with the indication of the onset of CPS.

As prototypical examples of nonlinear time-delay systems, we consider two specific models, namely (i) a piecewise linear time-delay system[44–46] and (ii) the Mackey–Glass time-delay system[32,47] and investigate the existence of CPS in the corresponding coupled systems.

A. Piecewise linear time-delay system

The following scalar first-order delay differential equation was introduced by Lu and He[44] and discussed in detail by Thangavel *et al.*,[45]

$$\dot{x}(t) = -ax(t) + bf(x(t-\tau)), \tag{1}$$

where a and b are parameters, τ is the time delay, and f is an odd piecewise linear function defined as

$$f(x) = \begin{cases} 0, & x \leq -4/3 \\ -1.5x - 2, & -4/3 < x \leq -0.8 \\ x, & -0.8 < x \leq 0.8 \\ -1.5x + 2, & 0.8 < x \leq 4/3 \\ 0, & x > 4/3. \end{cases} \tag{2}$$

Recently, we reported[46] that systems of the form (1) exhibit hyperchaotic behavior for suitable parametric values. For our present study, we find that for the choice of the
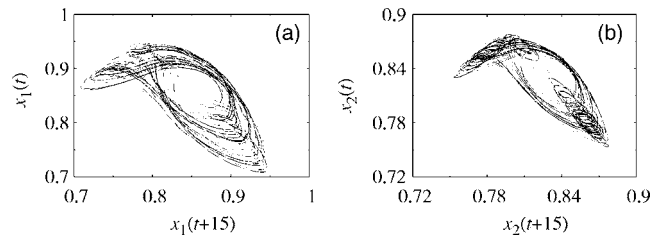

FIG. 1. (a) The non-phase-coherent hyperchaotic attractor of the drive [Eq. (4a)], and (b) the non-phase-coherent hyperchaotic attractor of the uncoupled response (4b)

parameters $a=1.0$, $b=1.2$, and $\tau=15.0$ with the initial condition $x(t)=0.9, t \in (-15,0)$, Eq. (1) exhibits hyperchaos. Detailed linear stability analysis, bifurcation analysis, and transient effects have been studied in Ref. 46. The corresponding pseudoattractor is shown in Fig. 1(a). The hyperchaotic nature of Eq. (1) is confirmed by the existence of multiple positive Lyapunov exponents. The first ten maximal Lyapunov exponents for the above choice of parameters as a function of delay time $\tau \in (2,29)$ are shown in Fig. 2(a) (the spectrum of Lyapunov exponents in this paper are calculated using the procedure suggested by Farmer[47]).

Studying synchronization in coupled systems of the form (1) is particularly appealing because of the facts that (i) system (1) exhibits a hyperchaotic attractor even for very small values of the delay time τ for appropriate values of the system parameters [the spectrum of Lyapunov exponents as a function of delay time τ is shown in Fig. 2(a)] and (ii) it is
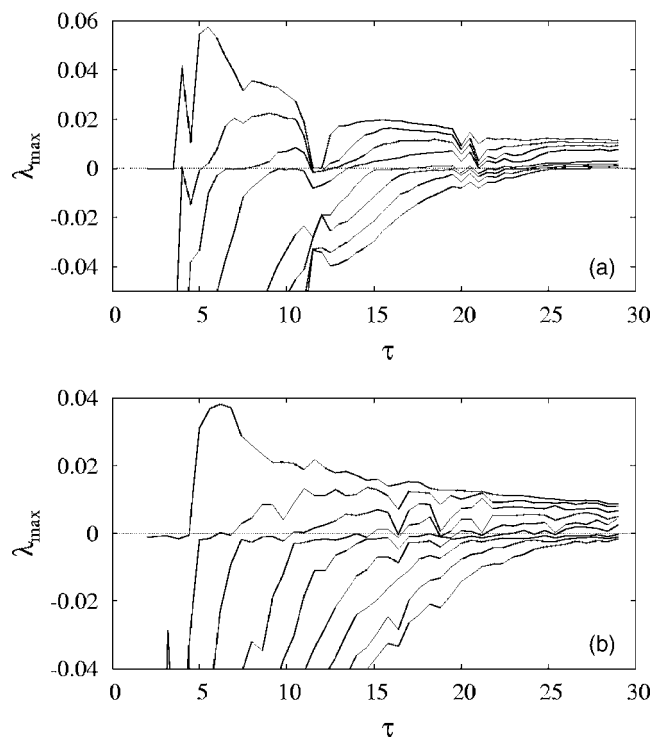

FIG. 2. The first ten maximal Lyapunov exponents λ_{max} of (a) the scalar time-delay system (1) and (2) or Eq. (4a) for the parameter values $a=1.0$, $b_1=1.2$, $\tau \in (2,29)$ and (b) the scalar time-delay system (4b) for the parameter values $a=1.0$, $b_1=1.1$ in the same range of delay time in the absence of the coupling b_3.

easily experimentally realizable as the piecewise linear function can be constructed readily and only low values of delay time are required for construction of a hyperchaotic attractor.

B. Mackey–Glass system

The second model we have used for the investigation of CPS is a model of blood production due to Mackey and Glass.[32] It is represented again by Eq. (1) but with the following functional form for $f(x)$:

$$f(x) = x(t-\tau)/(1.0 + x(t-\tau)^{10}). \tag{3}$$

Here, $x(t)$ represents the concentration of blood at time t, when it is produced, and $x(t-\tau)$ is the concentration when the "request" for more blood is made. In patients with leukemia, the time τ may become excessively large, and the concentration of blood will oscillate, or if τ is even larger, the concentration can vary chaotically, as demonstrated by Mackey and Glass.[32,47] This is a prototype model for delay systems exhibiting highly non-phase-coherent chaotic attractors and even hyperchaotic attractors for large value of delay time ($\tau > 28$). The pseudochaotic attractor of the Mackey–Glass system (1) and (3) for the standard parameter values $a = 0.1$, $b = 0.2$, and $\tau = 20$ with the initial condition $x(t) = 0.8, t \in (-20,0)$ is shown in Fig. 10(a) in Sec. IV below. The spectrum of Lyapunov exponents as a function of delay time $\tau \in (14,37)$ is shown in Fig. 9(a) (see Sec. IV below).

III. CPS IN COUPLED PIECEWISE-LINEAR TIME-DELAY SYSTEMS

We first consider the following unidirectionally coupled drive $x_1(t)$ and response $x_2(t)$ systems, which we have recently studied in detail in Refs. 48 and 49,

$$\dot{x}_1(t) = -ax_1(t) + b_1 f(x_1(t-\tau)), \tag{4a}$$

$$\dot{x}_2(t) = -ax_2(t) + b_2 f(x_2(t-\tau)) + b_3 f(x_1(t-\tau)), \tag{4b}$$

where b_1, b_2, and b_3 are constants, $a > 0$, τ is the delay time, and $f(x)$ is the piecewise linear function of the form (2).

We have chosen the values of parameters as (same values as studied in Ref. 37) $a = 1.0$, $b_1 = 1.2$, $b_2 = 1.1$, and $\tau = 15$. For this parametric choice, in the absence of coupling, the drive $x_1(t)$ and the response $x_2(t)$ systems evolve independently. Further in this case, both the drive $x_1(t)$ and the response $x_2(t)$ systems exhibit hyperchaotic attractors with five positive Lyapunov exponents and four positive Lyapunov exponents, respectively, i.e., both subsystems are qualitatively different (due to $b_1 \neq b_2$). The corresponding attractors are shown in Figs. 1(a) and 1(b), respectively, which clearly show the non-phase-coherent nature. The Kaplan and Yorke[47,50] dimension for the above attractors turns out to be 8.40 and 7.01, respectively, obtained by using the formula

$$D_L = j + \frac{\sum_{i=1}^{j} \lambda_i}{|\lambda_{j+1}|}, \tag{5}$$

where j is the largest integer for which $\lambda_1 + \ldots + \lambda_j \geq 0$. The parameter b_3 is the coupling strength of the unidirectional nonlinear coupling (4b), while the parameters
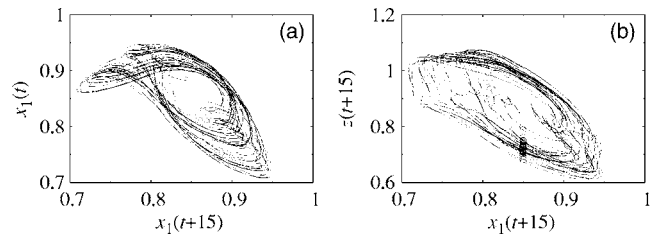

FIG. 3. (a) The non-phase-coherent hyperchaotic attractor of the uncoupled drive (4a) and (b) transformed attractor in the $x_1(t+\tau)$ and $z(t+\tau)$ space. Here the Poincaré points are represented as open circles.

b_1 and b_2 play the role of parameter mismatch resulting in nonidentical coupled time-delay systems. The spectrum of the first ten largest Lyapunov exponents of the uncoupled system (4a) for the values of the parameters $a = 1.0$ and $b_1 = 1.2$ in the range of time delay $\tau \in (2,29)$ is shown in Fig. 2(a) and that of the system (4b) for the parameter value $b_2 = 1.1$ in the same range of delay time is also shown in Fig. 2(b).

Now the task is to identify and to characterize the existence of CPS in the coupled time-delay systems (4), possessing highly non-phase-coherent hyperchaotic attractors, when the coupling is introduced ($b_3 > 0$). In the following, we present three different approaches to study CPS in coupled piecewise-linear time-delay systems (4).

A. CPS from Poincaré section of the transformed attractor [Fig. 3(b)]

We introduce a transformation to successfully capture the phase in the present problem. It transforms the non-phase coherent attractor [Fig. 3(a)] into a smeared limit cycle-like form with well-defined rotations around one center [Fig. 3(b)]. This transformation is performed by introducing the new state variable

$$z(t+\tau) = z(t+\tau,\hat{\tau}) = x_1(t)x_1(t+\hat{\tau})/x_1(t+\tau), \tag{6}$$

where $\hat{\tau}$ is the optimal value of delay time to be chosen (so as to rescale the original non-phase-coherent attractor into a smeared limit cycle-like form), and then we plot the above attractor [Fig. 3(a)] in the $(x_1(t+\tau), z(t+\tau))$ phase space. The functional form of this transformation (along with a delay time $\hat{\tau}$) has been identified by generalizing the transformation used in the case of chaotic attractors in the Lorenz system,[4] so as to unfold the original non-phase-coherent attractor [Fig. 3(a)] into a phase-coherent attractor. We find the optimal value of $\hat{\tau}$ for the attractor [Fig. 3(a)] of the piecewise linear time-delay system to be 1.6. It is to be noted that on closer examination of the transformed attractor [Fig. 3(b)] in the vicinity of the common center, it does not have any closed loop (unlike the case of the original attractor [Fig. 3(a)]) even though the trajectories show sharp turns in some regime of the phase space. If it is so, such closed loops will lead to phase mismatch, and one cannot obtain exact matching of phases of both the drive and response systems as shown in Fig. 4 and discussed below. Now the attractor [Fig. 3(b)] looks indeed like a smeared limit cycle with nearly well-defined rotations around a fixed center.
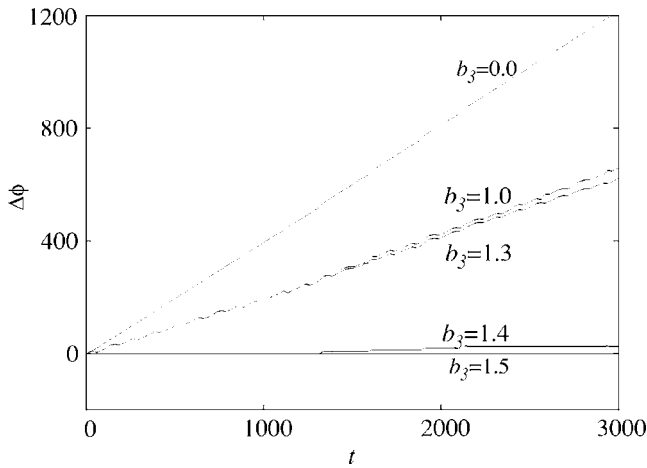
FIG. 4. Phase differences ($\Delta\phi = \phi_1^z(t) - \phi_2^z(t)$) between the systems (4a) and (4b) for different values of the coupling strength $b_3 = 0.0$, 1.0, 1.3, 1.4, and 1.5.

FIG. 5. (Color online) (a) Mean frequency ratio Ω_2/Ω_1 and their difference $\Delta\Omega = \Omega_2 - \Omega_1$ as a function of the coupling strength $b_3 \in (0,3)$ and (b) mutual information M as a function of coupling strength b_3.

It is to be noted that the above transformation (6) can be applied to the non-phase-coherent attractors of any time-delay system in general, except for the fact that the optimal value of $\hat{\tau}$ should be chosen for each system appropriately through trial and error by requiring the geometrical structure of the transformed attractor to have a fixed center of rotation. We have adopted here a geometric approach for the selection of $\hat{\tau}$ and look for an optimum transform that leads to a phase-coherent structure. This is indeed demonstrated for the attractor of the Mackey–Glass system in the next section. The motivation behind this transformation came from the transformation (A6), which is well known in the case of the Lorenz attractor discussed in the Appendix A. The main point that we want to stress here is that even for highly non-phase-coherent hyperchaotic attractors of time-delay systems, there is every possibility to identify suitable transformations of the type (6) to unfold the attractor and to identify phase as demonstrated in the above two typical cases of time-delay systems. One may ask a pertinent question here as to whether there exists a deeper underlying mathematical structure regarding such a transform. We do not have an answer to this question at present, and this remains an open problem.

Therefore, the phase of the transformed attractor can now be defined based on an appropriate Poincaré section which is transversally crossed by all trajectories using Eq. (A4) given in Appendix A. Open circles in Fig. 3(b) correspond to the Poincaré points of the smeared limit-cycle-like attractor. Phases, $\phi_1^z(t)$ and $\phi_2^z(t)$, of the drive $x_1(t)$ and the response $x_2(t)$ systems, respectively, are calculated from the state variables $z_1(t+\tau)$ and $z_2(t+\tau)$ according to Eq. (6). The existence of 1:1 CPS between the systems (4) is characterized by the phase-locking condition

$$|\phi_1^z(t) - \phi_2^z(t)| < \text{const.} \tag{7}$$

The phase differences ($\Delta\phi = \phi_1^z(t) - \phi_2^z(t)$) between the systems (4a) and (4b) are shown in Fig. 4 for different values of the coupling strength b_3. The phase difference $\Delta\phi$ between the systems (4a) and (4b) for $b_3 = 0.0$ (uncoupled) increases monotonically as a function of time, confirming that both systems are in an asynchronous state (also nonidentical) in
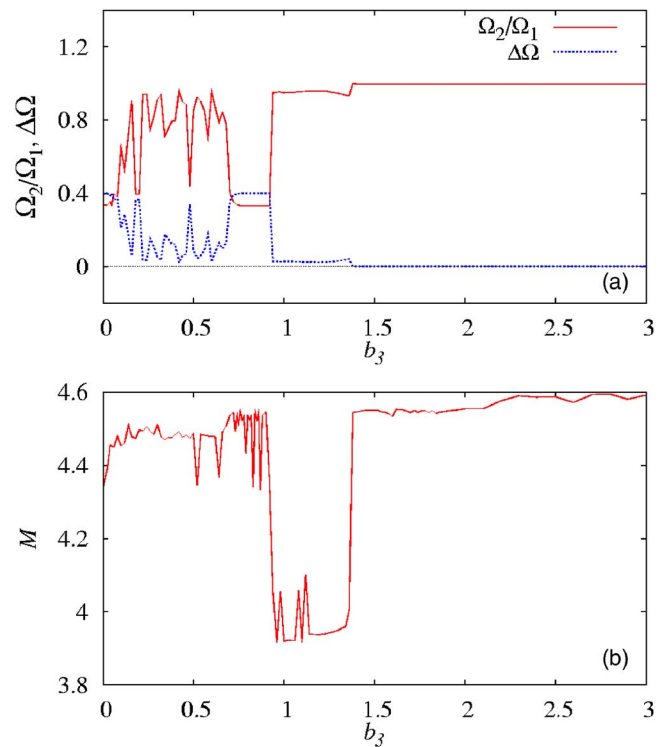
the absence of coupling between them. For the values of $b_3 = 1.0$ and 1.3, the phase slips in the corresponding phase difference $\Delta\phi$ show that the systems are in a transition state. The strong boundedness of the phase difference specified by Eq. (7) is obtained for $b_3 > 1.382$ and it becomes zero for the value of the coupling strength $b_3 = 1.5$, showing a high-quality CPS.

The mean frequency of the chaotic oscillations is defined as[14,22]

$$\Omega_{1,2} = \langle d\phi_{1,2}^z(t)/dt \rangle = \lim_{T\to\infty} \frac{1}{T} \int_0^T \dot{\phi}_{1,2}(t)dt, \tag{8}$$

and the 1:1 CPS between the drive $x_1(t)$ and the response $x_2(t)$ systems can also be characterized by a weaker condition of frequency locking, that is, the equality of their mean frequencies $\Omega_1 = \Omega_2$. The mean frequency ratio Ω_2/Ω_1 and its difference $\Delta\Omega = \Omega_2 - \Omega_1$ are shown in Fig. 5(a) as a function of the coupling strength $b_3 \in (0,3)$. It is also evident from this figure that the mean frequency locking criterion (8) is satisfied for $b_3 > 1.382$ from which both the frequency ratio Ω_2/Ω_1 and their difference $\Delta\Omega$ show substantial saturation in their values confirming the strong boundedness in the phases of both the systems.

The above results can be further strengthened by measuring the degree of PS quantitatively through the concept of mutual information between the cyclic phases,[43]

$$M = \sum_{i,j} p(i,j) \ln \frac{p(i,j)}{p_1(i)p_2(j)}, \qquad (9)$$

where $p_1(i)$ and $p_2(j)$ are the probabilities when the phases ϕ_1 and ϕ_2 are in the ith and jth bins, respectively, and $p(i,j)$ is the joint probability that ϕ_1 is in the ith bin and ϕ_2 in the jth bin. However, it is to be noted that mutual information between the phases can be used only to characterize the degree of PS provided phase has already been defined/known. Hence mutual information can be used only as an additional quantifier for measuring the degree of phase synchronization. Mutual information M as a function of coupling strength $b_3 \in (0,3)$ is shown in Fig. 5(b), which clearly indicates the high degree of PS for $b_3 > 1.382$ in good agreement with the frequency ratio Ω_2/Ω_1 and their difference $\Delta\Omega$ shown in Fig. 5(a).

B. CPS from recurrence quantification analysis

The complex synchronization phenomena in the coupled time-delay systems (4) can also be analyzed by means of the very recently proposed methods based on recurrence plots.[39,51] These methods help to identify and quantify CPS (particularly in non-phase-coherent attractors) and GS.

For this purpose, the generalized autocorrelation function $P(t)$ has been introduced in Refs. 39 and 51 as

$$P(t) = \frac{1}{N-t} \sum_{i=1}^{N-t} \Theta(\epsilon - \|X_i - X_{i+t}\|), \qquad (10)$$

where Θ is the Heaviside function, X_i is the ith data corresponding to either the drive variable x_1 or the response variable x_2 specified by Eqs. (4), and ϵ is a predefined threshold. $\|\cdot\|$ is the Euclidean norm and N is the number of data points. $P(t)$ can be considered as a statistical measure of how often ϕ has increased by 2π or multiples of 2π within the time t in the original space. If two systems are in CPS, their phases increase on average by $K.2\pi$, where K is a natural number, within the same time interval t. The value of K corresponds to the number of cycles when $\|X(t+T)-X(t)\| \sim 0$, or equivalently when $\|X(t+T)-X(t)\| < \epsilon$, where T is the period of the system. Hence, looking at the coincidence of the positions of the maxima of $P(t)$ for both systems, one can qualitatively identify CPS.

A criterion to quantify CPS is the cross-correlation coefficient between the drive, $P_1(t)$, and the response, $P_2(t)$, which can be defined as the Correlation of Probability of Recurrence (CPR)

$$\text{CPR} = \langle \overline{P_1}(t) \overline{P_2}(t) \rangle / \sigma_1 \sigma_2, \qquad (11)$$

where $\overline{P}_{1,2}$ means that the mean value has been subtracted and $\sigma_{1,2}$ are the standard deviations of $P_1(t)$ and $P_2(t)$, respectively. If both systems are in CPS, the probability of recurrence is maximal at the same time t and $\text{CPR} \approx 1$. If they are not in CPS, the maxima do not occur simultaneously and hence one can expect a drift in both the probability of recurrences and low values of CPR.

When the systems (4) are in generalized synchronization, two close states in the phase space of the drive variable correspond to that of the response. Hence the neighborhood identity is preserved in phase space. Since the recurrence plots are merely a record of the neighborhood of each point in the phase space, one can expect that their respective recurrence plots are almost identical. Based on these facts, two indices are defined to quantify GS.

First, the authors of Ref. 51 proposed the Joint Probability of Recurrences (JPR),

$$\text{JPR} = \frac{\frac{1}{N^2} \sum_{i,j}^{N} \Theta(\epsilon_x - \|X_i - X_j\|)\Theta(\epsilon_y - \|Y_i - Y_j\|) - RR}{1 - RR}, \qquad (12)$$

where RR is the rate of recurrence, ϵ_x and ϵ_y are thresholds corresponding to the drive and response systems, respectively, and X_i is the ith data corresponding to the drive variable x_1 and Y_i is the ith data corresponding to the response variable x_2 specified by Eqs. (4). RR measures the density of recurrence points and it is fixed as 0.02.[51] JPR is close to 1 for systems in GS and is small when they are not in GS. The second index depends on the coincidence of the probability of recurrence, which is defined as the Similarity of Probability of Recurrence (SPR),

$$\text{SPR} = 1 - \langle (\overline{P_1}(t) - \overline{P_2}(t))^2 \rangle / \sigma_1 \sigma_2. \qquad (13)$$

SPR is of order 1 if both systems are in GS and approximately zero or negative if they evolve independently.

Now, we will apply these concepts to the original (non-transformed) attractor [Fig. 3(a)]. We estimate these recurrence-based measures from 5000 data points after sufficient transients with the integration step $h=0.01$ and sampling rate $\Delta t = 100$. The generalized autocorrelation functions $P_1(t)$ and $P_2(t)$ [Fig. 6(a)] for the coupling $b_3 = 0.6$ show that the maxima of both systems do not occur simultaneously and there exists a drift between them, so there is no synchronization at all. This is also reflected in the rather low value of $\text{CPR} = 0.381$. For $b_3 \in (0.78, 1.381)$, from Fig. 7 we observe the first substantial increase of recurrence reaching CPR $\approx 0.5 - 0.6$. Looking into the details of the generalized correlation functions $P(t)$, we find that now the main oscillatory dynamics becomes locked, i.e., the main maxima of P_1 and P_2 coincide. For $b_3 \in (1.382, 2.2)$, CPR reaches almost 1 as seen in Fig. 7, while now the positions of all maxima of P_1 and P_2 are also in agreement and this is in accordance with the strongly bounded nature of phase differences. This is a strong indication for CPS. Note, however, that the heights of the peaks are clearly different [Fig. 6(b)]. The differences in the peak heights indicate that there is no strong interrelation in the amplitudes. Further increase of the coupling (here $b_3 = 2.21$) leads to the coincidence of both the positions and the heights of the peaks [Fig. 6(c)] referring to GS in systems (4). This is also confirmed from the maximal values of the indices $\text{JPR} = 1$ and $\text{SPR} = 1$, which is due to the strong correlation in the amplitudes of both systems. It is clear from the construction of SPR that it measures the similarity between the generalized autocorrelation functions $P_1(t)$ and $P_2(t)$. In the regimes of CPS, as the generalized autocorrelation functions coincide in almost all the regimes except for the height of its maxima, it is also quantified by larger values of SPR. The index SPR in Fig. 7 also shows the onset of CPS
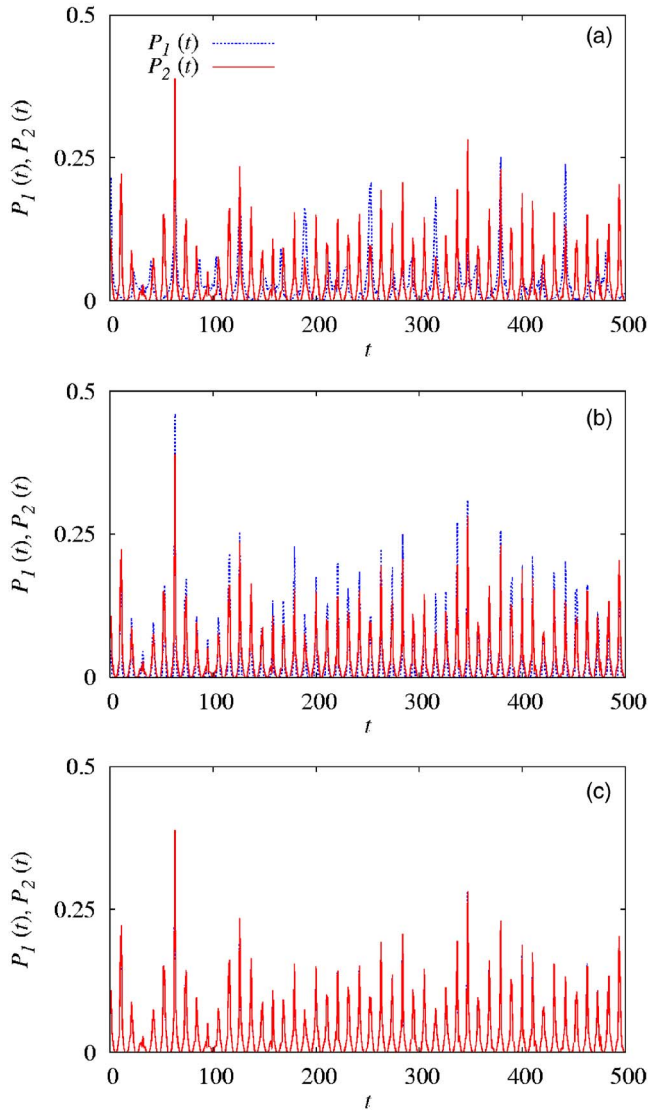
FIG. 6. (Color online) Generalized autocorrelation functions of both the drive $P_1(t)$ and the response $P_2(t)$ systems. (a) Non-phase-synchronization for $b_3=0.6$, (b) phase synchronization for $b_3=1.5$, and (c) generalized synchronization for $b_3=2.3$.

and it fluctuates around the value 1 in the regime of CPS ($b_3 \in (1.382, 2.2)$) before reaching saturation, confirming the strong correlation in the amplitudes of both the systems, thereby quantifying the existence of GS. The transition from
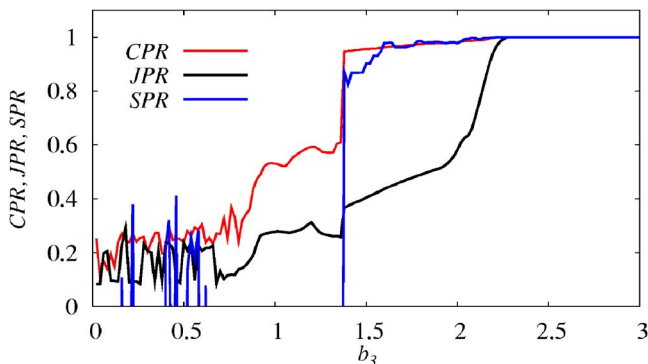

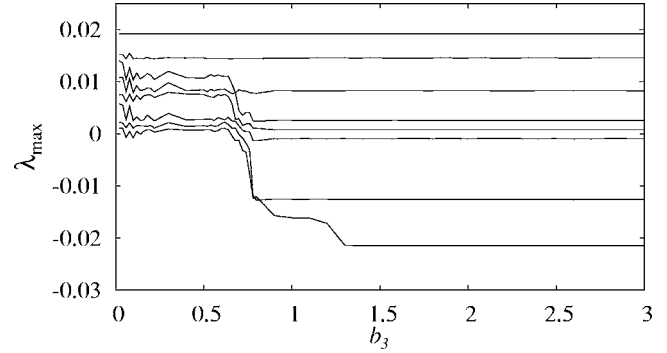FIG. 7. (Color online) Indices CPR, JPR, and SPR as a function of coupling strength $b_3 \in (0,3)$.

FIG. 8. Spectrum of the first eight largest Lyapunov exponents of the coupled systems (4) as a function of coupling strength $b_3 \in (0,3)$.

nonsynchronized state via CPS to GS is characterized by the maximal values of CPR, SPR, and JPR (Fig. 7). As expected from the construction of these functions, CPR refers mainly to the onset of CPS, whereas JPR quantifies clearly the onset of GS, and SPR indicates both the onset of CPS and GS. In this connection, we have also confirmed the onset and existence of GS by using the auxiliary system approach[52] introduced by Abarbanel *et al.* for the range of the coupling strength $b_3 > 2.2$.

C. CPS from the spectrum of Lyapunov exponents

The transition from nonsynchronization to CPS is also characterized by changes in the Lyapunov exponents of the coupled time-delay systems (4). The spectrum of the eight largest Lyapunov exponents of the coupled systems is shown in Fig. 8. From this figure, one can find that all the positive Lyapunov exponents, except the largest one ($\lambda_{max}^{(2)}$), corresponding to the response system suddenly become negative at the value of the coupling strength $b_3=0.78$, which is an indication of the onset of transition regime. One may also note that at this value of b_3, already one of the Lyapunov exponents of the response system attains negative saturation while the another one reaches negative saturation slightly above $b_3=0.78$. This is a strong indication that in this rather complex attractor, the amplitudes become somewhat interrelated already at the transition to CPS (as in the funnel attractor[38] of the Rössler system). Also the third positive Lyapunov exponent of the response system gradually becomes more negative from $b_3=0.78$ and reaches its saturation value at $b_3=1.381$, confirming the onset of CPS [which is also indicated by the transition of the indices of CPR and SPR in Fig. 7 in the range of $b_3 \in (0.78, 1.381)$]. It is interesting to note that the Lyapunov exponents of the response system $\lambda_i^{(2)}$ [other than $\lambda_{max}^{(2)}$] are changing already at the early stage of CPS ($b_3 \in (0.78, 1.381)$), where the complete CPS is not yet attained. This has also been observed for the onset of CPS in phase-coherent and non-phase-coherent oscillators without time-delay.[11,22,54]

IV. CPS IN COUPLED MACKEY–GLASS SYSTEMS

In this section, we will bring out the existence of CPS in coupled Mackey–Glass systems of the form
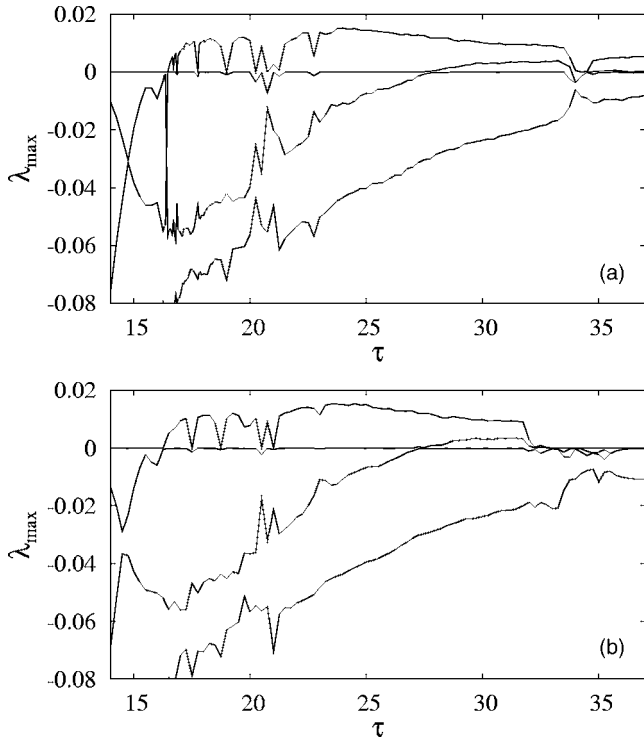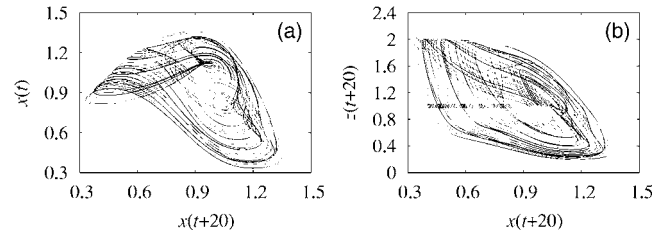
FIG. 10. (a) The non-phase-coherent chaotic attractor of the uncoupled drive (14a) and (b) transformed attractor in the $x_1(t+\tau)$ and $z(t+\tau)$ space along with the Poincaré points represented as open circles.

A. CPS from Poincaré section of the transformed attractor [Fig. 10(b)]

The non-phase-coherent chaotic attractor [Fig. 10(a)] of the Mackey-Glass system is transformed into a smeared limit cycle-like attractor [Fig. 10(b)] using the same transformation (6) as used for the piecewise-linear time-delay systems. For the attractor [Fig. 10(a)] of the Mackey–Glass system, the optimal value of the delay time $\hat{\tau}$ in Eq. (6) is found to be 8.0. The Poincaré points are shown as open circles in Fig. 10(b), from which the instantaneous phase $\phi_1^z(t)$ is calculated using Eq. (A4). The existence of CPS in the coupled Mackey–Glass systems (14) is also characterized by the phase-locking condition (7) as shown in Fig. 11. The phase differences $\Delta\phi = \phi_1^z(t) - \phi_2^z(t)$ between the systems (14a) and (14b) for the values of the coupling strength $b_3 = 0.04$, 0.08, 0.11, 0.12, and 0.3 are shown in Fig. 11. For the value of the coupling strength $b_3 = 0.3$, there exists a strong boundedness in the phase difference showing high-quality CPS. The mean frequency ratio Ω_2/Ω_1 calculated from Eq. (8) along with the mean frequency difference $\Delta\Omega$ is shown in Fig. 12(a). The value of mean frequency ratio $\Omega_2/\Omega_1 \approx 1$ in the range of $b_3 \in (0.12, 0.23)$ corresponding to the transition regime (which is also to be confirmed from the indices CPR and JPR in the next subsection); see the inset of Fig. 12(a). Similarly, the mean frequency difference is also $\Delta\Omega \approx 0$, confirming the transition regime. For the value of $b_3 > 0.23$, both quantities Ω_2/Ω_1 and $\Delta\Omega$ acquire the complete saturation in their values confirming the existence of CPS. Further, the mutual

FIG. 9. The first four maximal Lyapunov exponents λ_{max} of (a) the Mackey–Glass time-delay system (14a) for the parameter values $a=0.1$, $b_1=0.2$, $\tau \in (14, 37)$ and (b) time-delay system (14b) for the parameter values $a=0.1$, $b_1=0.205$ in the same range of delay time in the absence of the coupling b_3.

$$\dot{x}_1(t) = -ax_1(t) + b_1 x_1(t-\tau)/(1.0 + x_1(t-\tau)^{10}), \qquad (14a)$$

$$\dot{x}_2(t) = -ax_2(t) + b_2 x_2(t-\tau)/(1.0 + x_2(t-\tau)^{10}) + b_3 x_1(t-\tau)/$$
$$(1.0 + x_1(t-\tau)^{10}), \qquad (14b)$$

where a, b_1, b_2 are constants, b_3 is the coupling parameter, and τ is the delay time.

We have chosen the parameter values (cf. Refs. 32 and 47) as $a=0.1$, $b_1=0.2$, $b_2=0.205$, $\tau=20$, and we varied the coupling strength b_3. The non-phase-coherent chaotic attractor of the system $x_1(t)$, Eq. (14a), for the above choice of parameters is shown in Fig. 10(a) and it possesses one positive and one zero Lyapunov exponent. Similarly, the second system $x_2(t)$, Eq. (14b), also exhibits a non-phase-coherent chaotic attractor with one positive and one zero Lyapunov exponent for the chosen parametric values in the absence of the coupling strength b_3. The parameters b_1 and b_2 contribute to the parameter mismatch between the systems $x_1(t)$ and $x_2(t)$. The spectrum of the first four maximal Lyapunov exponents of both systems (14a) and (14b) is shown in Figs. 9(a) and 9(b), respectively, as a function of delay time $\tau \in (14, 37)$ when $b_3=0$. The Kaplan and Yorke[47,50] dimension calculated using Eq. (5) for the present systems [Eqs. (14a) and (14b)] works out to be 2.279 69 and 2.210 96, respectively. Now, the existence of CPS as a function of the coupling strength in the coupled Mackey–Glass systems (14) will be discussed using the above three approaches used for identifying CPS in coupled piecewise-linear time-delay systems (4).
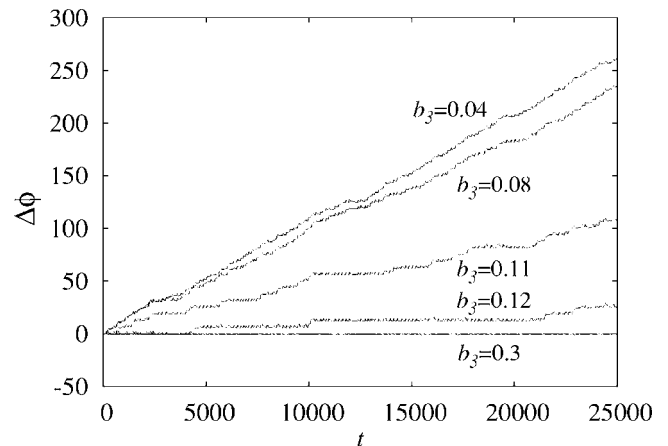

FIG. 11. Phase differences ($\Delta\phi = \phi_1^z(t) - \phi_2^z(t)$) between the systems (14a) and (14b) for different values of the coupling strength $b_3 = 0.04$, 0.08, 0.11, 0.12, and 0.3.
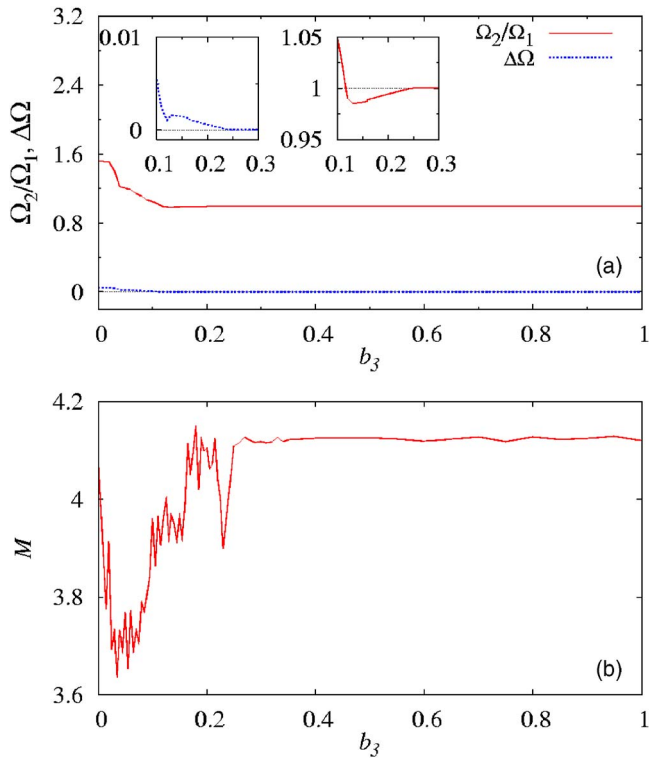
FIG. 12. (Color online) (a) Mean frequency ratio Ω_2/Ω_1 and their difference $\Delta\Omega = \Omega_2 - \Omega_1$ as a function of the coupling strength $b_3 \in (0,1)$ and (b) mutual information M as a function of coupling strength b_3.

information calculated using Eq. (9) clearly indicates the increase in the degree of PS for the value of coupling strength $b_3 > 0.23$ as shown in Fig. 12(b), which is also in agreement with the frequency ratio Ω_2/Ω_1 and the mean frequency difference $\Delta\Omega$ shown in Fig. 12(b).

B. CPS from recurrence quantification analysis

The existence of CPS from the original non-phase-coherent chaotic attractors of the systems (14) is analyzed in this section using the recurrence quantification measures defined in Sec. II B. We have estimated these measures again using a set of 5000 data points, and the same integration step and the sampling rate as used in the case of coupled piecewise-linear time-delay systems (4). The maxima of generalized autocorrelations of both the drive $P_1(t)$ and the response $P_2(t)$ systems [Fig. 13(a)] do not occur simultaneously for $b_3 = 0.1$, which indicates the independent evolution of both the systems without any correlation, and this is also reflected in the rather low value of CPR=0.4. For $b_3 = 0.3$, the maxima of both $P_1(t)$ and $P_2(t)$ are in good agreement [Fig. 13(b)] and this shows the strongly bounded phase difference. It is to be noted that even though both of the maxima coincide, the heights of the peaks are clearly of different magnitudes contributing to the fact that there is no strong correlation in the amplitudes of both the systems indicating CPS. Both the positions and the peaks are in coincidence [Fig. 13(c)] for the value of coupling strength $b_3 = 0.9$ in accordance with the strong correlation in the amplitudes of both the systems (14) corresponding to GS. This is also reflected in the maximal values of both JPR=1 and
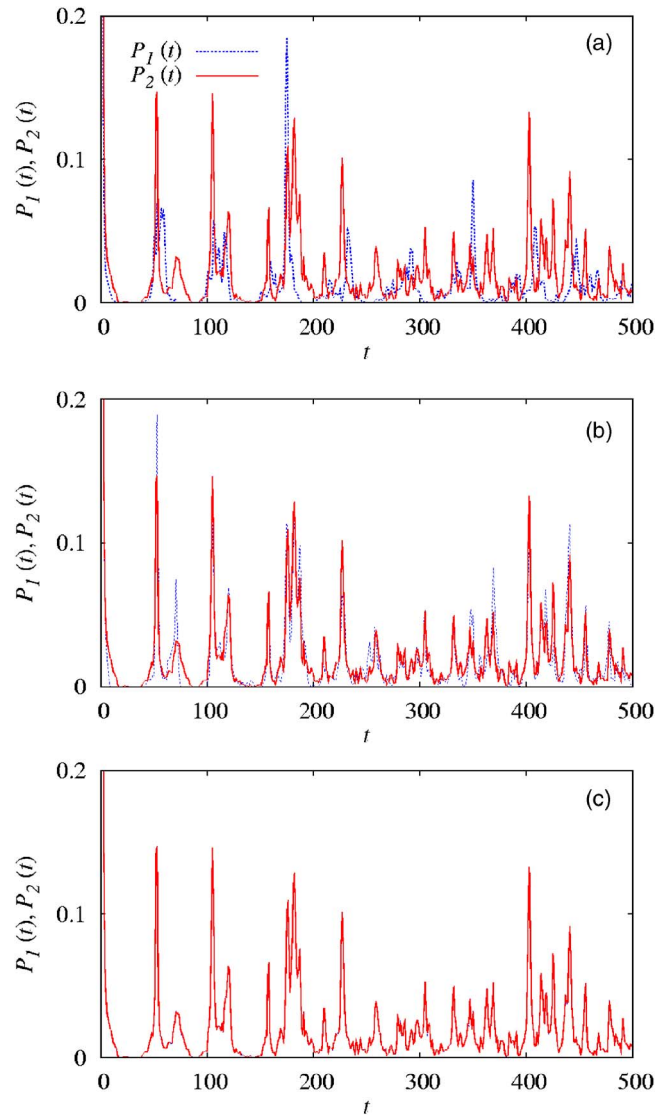

FIG. 13. (Color online) Generalized autocorrelation functions of both the drive system (14a), $P_1(t)$, and the response system (14b), $P_2(t)$. (a) Non-phase-synchronization for $b_3 = 0.1$, (b) phase synchronization for $b_3 = 0.3$, and (c) generalized synchronization for $b_3 = 0.9$.

SPR=1. The spectra of CPR, JPR, and SPR are shown in Fig. 14. The onset of CPS is shown by the first substantial increase of the index CPR at $b_3 = 0.11$ and the transition regime is shown by the successive plateaus of CPR in the
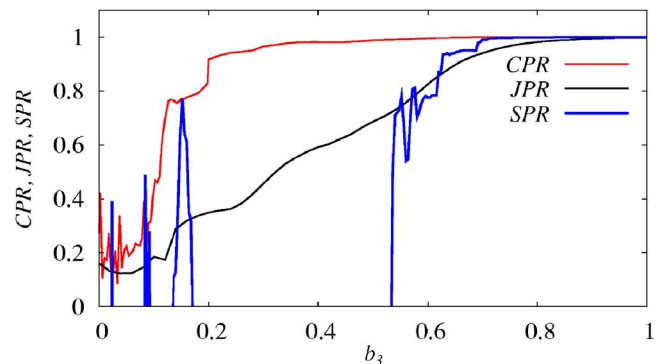

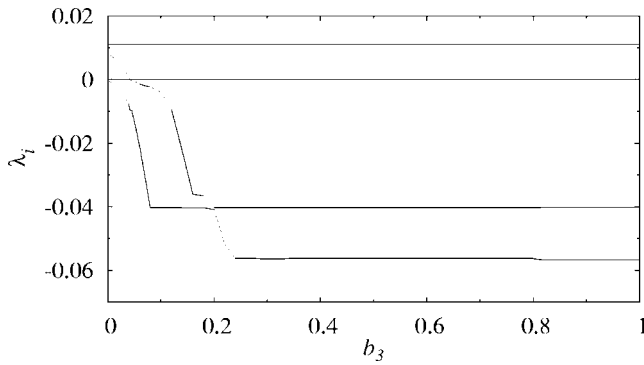FIG. 14. (Color online) Indices CPR, JPR, and SPR as a function of coupling strength $b_3 \in (0,1)$.

FIG. 15. Spectrum of the first four largest Lyapunov exponents of the coupled systems (14) as a function of coupling strength $b_3 \in (0,1)$.

range $b_3 \in (0.12, 0.23)$. The maximal values of CPR for b_3 > 0.23 indeed confirm the existence of high-quality CPS. The existence of GS is also confirmed from both the indices JPR and SPR.

C. CPS from the spectrum of Lyapunov exponents

The onset of CPS is also characterized by the changes in the spectrum of Lyapunov exponents of the coupled Mackey–Glass systems (14). The spectrum of the first four largest Lyapunov exponents of the coupled systems (14) is shown in Fig. 15. The zero Lyapunov exponent of the response system $x_2(t)$ already becomes negative as soon as the coupling is introduced and the onset of CPS is indicated by the negative saturation of the zero Lyapunov exponent at $b_3 = 0.11$. The positive Lyapunov exponent of the response system becomes gradually negative in the transition regime ($b_3 \in (0.12, 0.23)$) and it reaches its negative saturation at $b_3 = 0.23$, at which high-quality CPS exists. The transition of the positive Lyapunov exponent to negativity in this rather complex attractor is again a firm indication of some degree of correlation in the amplitudes of both systems even before the onset of CPS. As noted earlier, this behavior of negative transition of the positive Lyapunov exponent of the response system before CPS has also been observed in Refs. 11, 22, 53, and 54.

V. SUMMARY AND CONCLUSION

We have identified and characterized the existence of CPS in both the coupled piecewise-linear time-delay systems and in the coupled Mackey–Glass systems possessing highly non-phase-coherent chaotic attractors. We have shown that there is a typical transition from a nonsynchronized state to CPS and subsequently to GS as a function of the coupling strength in both systems. Similar results are obtained for different sampling intervals Δt and for various values of delay time τ.

We have introduced a suitable transformation, which works equally well for both the systems possessing characteristically distinct attractors (hyperchaotic attractor in the piecewise linear time-delay system and chaotic attractor in the Mackey–Glass system), to capture the phase of the underling non-phase-coherent attractor. Both the phase- and the frequency-locking criteria are satisfied by the instantaneous

phases calculated from the transformed attractors in both the piecewise-linear and the Mackey–Glass time-delay systems. The frequency ratio and its difference as a function of coupling strength clearly show the onset of CPS in both cases. We have also characterized the existence of CPS and GS in terms of recurrence-based indices, namely generalized autocorrelation function $P(t)$, CPR, JPR, and SPR, and we quantified the different synchronization regimes in terms of them. The onset of CPS and GS is also clearly shown by the spectra of CPR, JPR, and SPR. The above transition is also confirmed by the changes in the spectrum of Lyapunov exponents. The recurrence-based technique as well as the new transformation are also appropriate for the analysis of experimental data, and we are now investigating the experimental verification of these findings in nonlinear electronic circuits and in biological systems. Also, the recurrence-based indices are found to be more appropriate for identifying the existence and analysis of synchronizations, in particular CPS, and their onset in the case of nonlinear time-delay systems in general, where very often the attractor is non-phase-coherent and high-dimensional. It should also be emphasized that the recurrence-based measures are more efficient than other nonlinear techniques[39] such as mutual information, predictability, etc. These measures have a high potential for applications, and we are also investigating the possibility of extending these techniques to complex networks.

APPENDIX A: CPS IN CHAOTIC SYSTEMS: PHASE-COHERENT AND NON-PHASE-COHERENT ATTRACTORS

Definition of CPS in coupled chaotic systems is derived from the classical definition of phase synchronization in periodic oscillators. Interacting chaotic systems are said to be in a phase-synchronized state when there exists entrainment between phases of the systems, while their amplitudes may remain chaotic and uncorrelated. In other words, CPS exists when their respective frequencies and phases are locked.[1,4,14] To study CPS, one has to identify a well-defined phase variable in both coupled systems. If the flow of the chaotic oscillators has a proper rotation around a certain reference point, the phase can be defined in a straightforward way. In this case, the corresponding attractor is referred to as a phase-coherent attractor in the literature[1,4,14,17,37,38] and the phase can be introduced straightforwardly as[1,4]

$$\phi(t) = \arctan(y(t)/x(t)). \tag{A1}$$

A more general approach to define the phase in chaotic oscillators is the analytic signal approach[1,4] introduced in Ref. 55. The analytic signal $\chi(t)$ is given by
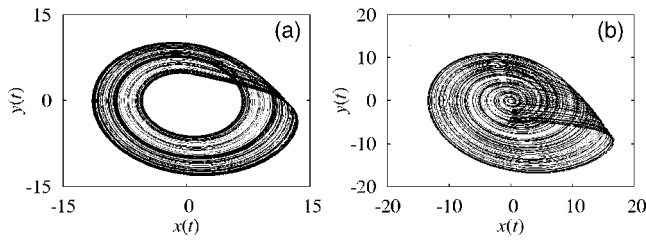
FIG. 16. Phase-coherent and funnel (non-phase-coherent) Rössler attractors with parameters (a) $a=0.15$ and (b) $a=0.25$.

$$\chi(t) = s(t) + i\tilde{s}(t) = A(t)\exp^{i\Phi(t)}, \tag{A2}$$

where $\tilde{s}(t)$ denotes the Hilbert transform of the observed scalar time series $s(t)$,

$$\tilde{s}(t) = \frac{1}{\pi}\text{P.V.}\int_{-\infty}^{\infty}\frac{s(t')}{t-t'}dt', \tag{A3}$$

where P.V. stands for the Cauchy principle value of the integral, and this method is especially useful for experimental applications.[1,4]

The phase of a chaotic attractor can also be defined based on an appropriate Poincaré section which the chaotic trajectory crosses once for each rotation. Each crossing of the orbit with the Poincaré section corresponds to an increment of 2π of the phase, and the phase in between two crosses is linearly interpolated,[1,4]

$$\Phi(t) = 2\pi k + 2\pi\frac{t-t_k}{t_{k+1}-t_k}, \quad (t_k < t < t_{k+1}), \tag{A4}$$

where t_k is the time of kth crossing of the flow with the Poincaré section. For the phase-coherent chaotic oscillators, that is, for flows that have a proper rotation around a certain reference point, the phases calculated by these three different ways are in good agreement.[1,4]

As a typical example, consider the Rössler system,

$$\dot{x} = -y - z, \tag{A5a}$$

$$\dot{y} = x + ay, \tag{A5b}$$

$$\dot{z} = 0.2 + z(x - 8.5). \tag{A5c}$$

The topology of the attractor of the Rössler system is determined by the parameter a. For $a=0.15$, a phase-coherent attractor [see Fig. 16(a)] is observed with rather simple topological properties[56,57] [where the projection of the chaotic attractor on the (x,y) plane looks like a smeared limit cycle with the phase point always rotated around a fixed origin with monotonically increasing phase] and hence the phase can be calculated straightforwardly as discussed above.

However, in chaotic dynamics one often encounters non-phase-coherent attractors where the flows are without a proper rotation around a fixed reference point (with the origin coinciding with the center of rotation), in which case a single characteristic time scale does not exist in general. In such circumstances, it is difficult or impossible to find a proper center of rotation and it is also intricate to find a Poincaré section that is crossed transversally by all trajectories of the chaotic attractor. As a consequence, such a non-phase-coherent chaotic attractor is not characterized by a monotonically increasing phase. Hence the phase of such a non-phase-coherent attractor cannot be defined straightforwardly as in the case of phase-coherent attractor. Therefore, the above definitions of phase are no longer applicable for non-phase-coherent chaotic attractors. So specialized techniques/tools have to be identified to introduce phase in non-phase-coherent attractors.

It has also been demonstrated that certain non-phase-coherent chaotic attractors can be transformed into smeared limit-cycle-like attractors by introducing a suitable transformation of the original variables. For example, in the case of a Lorenz attractor, a transformation of the form

$$u(t) = \sqrt{x^2 + y^2} \tag{A6}$$

is introduced[1] and the projected trajectory in the plane (u,z) resembles that of the Rössler attractor. Now phase of the respective attractor is introduced using the above approaches for phase-coherent attractors.

However, such a transformation does not always exist or can be found in the case of non-phase-coherent attractors in general. Again, as a typical example consider the Rössler system specified by Eq. (A5). The topology of the Rössler attractor changes dramatically if the parameter a exceeds 0.21 and the phase in this case is not well defined. The funnel (non-phase-coherent) attractor for the value $a=0.25$ is shown in Fig. 16(b). There are large and small loops [see Fig. 16(b)] on the (x,y) plane and it is not evident which phase gain should be attributed to these loops and hence phase cannot be calculated simply as in the case of a phase-coherent chaotic attractor [Fig. 16(a)] or through simple transformations. Therefore, recently another definition of the phase based on the general idea of the curvature has been proposed by Osipov et al.[38] For any two-dimensional curve $\mathbf{r}=(u,v)$ the angle velocity at each point is

$$\nu = (ds/dt)/R,$$

where $ds/dt = \sqrt{\dot{u}^2 + \dot{v}^2}$ is the speed along the curve and $R = (\dot{u}^2 + \dot{v}^2)^{3/2}/(\dot{v}\ddot{u} - \ddot{v}\dot{u})$ is the radius of the curvature. If $R > 0$ at each point, then

$$\nu = \frac{d\Phi}{dt} = \frac{\dot{v}\ddot{u} - \ddot{v}\dot{u}}{\dot{u}^2 + \dot{v}^2}$$

is always positive and hence the variable

$$\Phi = \int \nu dt = \arctan\frac{\dot{v}}{\dot{u}} \tag{A7}$$

is a monotonically increasing function of time and can be considered as the phase of the oscillator. These definitions of frequency and phase are general for any dynamical system if the projection of the phase trajectory on some plane is a curve with a positive curvature. Now for the non-phase-coherent Rössler attractor in the funnel regime, the projections of chaotic trajectories on the plane $(\dot{x},\dot{y})$ always rotate around the origin, and the phase can be defined as $\Phi = \arctan(\dot{y}/\dot{x})$.[38] However, it is not clear whether an appropriate plane can always be found on which the projected trajec-

tories rotate around the origin for higher-dimensional chaotic systems, as such systems will very often exhibit more complicated attractors with more than one positive Lyapunov exponent as in the case of typical time-delay systems discussed in the main part of this paper.

[1] S. Boccaletti, J. Kurths, G. Osipov, D. L. Valladares, and C. S. Zhou, Phys. Rep. **366**, 1 (2002).
[2] Special issue on phase synchronization edited by J. Kurths, Int. J. Bifurcation Chaos Appl. Sci. Eng. 10 (2000).
[3] Special focus issue on chaotic synchronization edited by L. Pecora, Chaos 7 (1997).
[4] A. S. Pikovsky, M. G. Rosenblum, and J. Kurths, *Synchronization-A Unified Approach to Nonlinear Science* (Cambridge University Press, Cambridge, 2001).
[5] H. Fujisaka and T. Yamada, Prog. Theor. Phys. **69**, 32 (1983).
[6] L. M. Pecora and T. L. Carroll, Phys. Rev. Lett. **64**, 821 (1990).
[7] A. S. Pikovsky, Z. Phys. B: Condens. Matter **55**, 149 (1984).
[8] L. M. Pecora and T. L. Carroll, Chaos **7**, 520 (1997).
[9] N. F. Rulkov, M. M. Sushchik, L. S. Tsimring, and H. D. I. Abarbanel, Phys. Rev. E **51**, 980 (1995).
[10] L. Kocarev and U. Parlitz, Phys. Rev. Lett. **76**, 1816 (1996).
[11] M. G. Rosenblum, A. S. Pikovsky, and J. Kurths, Phys. Rev. Lett. **76**, 1804 (1996).
[12] T. Yalcinkaya and Y. C. Lai, Phys. Rev. Lett. **79**, 3885 (1997).
[13] Y. C. Lai, Phys. Rev. E **58**, R6911 (1998).
[14] G. V. Osipov, A. S. Pikovsky, M. G. Rosenblum, and J. Kurths, Phys. Rev. E **55**, 2353 (1997).
[15] A. S. Pikovsky, G. Osipov, M. G. Rosenblum, M. Zaks, and J. Kurths, Phys. Rev. Lett. **79**, 47 (1997).
[16] A. S. Pikovsky, M. G. Rosenblum, G. Osipov, and J. Kurths, Physica D **219**, 104 (1997).
[17] M. G. Rosenblum, A. S. Pikovsky, and J. Kurths, Phys. Rev. Lett. **78**, 4193 (1997).
[18] U. Parlitz, L. Junge, W. Lauterborn, and L. Kocarev, Phys. Rev. E **54**, 2115 (1996).
[19] M. Zhan, G. W. Wei, and C. H. Lai, Phys. Rev. E **65**, 036202 (2002).
[20] M. Zhan, Z. G. Zheng, G. Hu, and X. H. Peng, Phys. Rev. E **62**, 3552 (2000).
[21] E. Rosa, C. M. Ticos, W. B. Pardo, J. A. Walkenstein, M. Monti, and J. Kurths, Phys. Rev. E **68**, 025202(R) (2003).
[22] S. Guan, C. H. Lai, and G. W. Wei, Phys. Rev. E **72**, 016205 (2005).
[23] A. Pujol-Peré, O. Calvo, M. A. Matias, and J. Kurths, Chaos **13**, 319 (2003).
[24] M. S. Baptista, T. P. Silva, J. C. Sartorelli, I. L. Caldas, and E. Rosa, Phys. Rev. E **67**, 056212 (2003).
[25] S. K. Dana, B. Blasius, and J. Kurths, Chaos **16**, 023111 (2006).
[26] K. V. Volodohenko, V. N. Ivanov, S. H. Gong, M. Choi, Y. J. Park, and C. M. Kim, Opt. Lett. **26**, 1406 (2001).
[27] D. J. DeShazer, R. Breban, E. Ott, and R. Roy, Phys. Rev. Lett. **87**, 044101 (2001).
[28] D. Maza, A. Vallone, H. Mancini, and S. Boccaletti, Phys. Rev. Lett. **85**, 5567 (2000).
[29] P. Tass, M. G. Rosenblum, J. Weule, J. Kurths, A. Pikovsky, J. Volkmann, A. Schnitzler, and H. J. Freund, Phys. Rev. Lett. **81**, 3291 (1998).
[30] R. C. Elson, A. I. Selverston, R. Huerta, N. F. Rulkov, M. I. Rabinovich, and H. D. I. Abarbanel, Phys. Rev. Lett. **81**, 5692 (1998).
[31] D. Maraun and J. Kurths, Geophys. Res. Lett. **32**, L15709 (2005).
[32] M. C. Mackey and L. Glass, Science **197**, 287 (1977).
[33] T. Heil, I. Fischer, W. Elsasser, B. Krauskopf, K. Green, and A. Gavrielides, Phys. Rev. E **67**, 066214 (2003).
[34] N. Kopell, G. B. Ermentrout, M. A. Whittington, and R. D. Traub, Proc. Natl. Acad. Sci. U.S.A. **97**, 1867 (2000).
[35] L. B. Shaw, I. B. Schwartz, E. A. Rogers, and R. Roy, Chaos **16**, 015111 (2006).
[36] M. Kostur, P. Hanggi, P. Talkner, and J. L. Mateos, Phys. Rev. E **72**, 036210 (2005).
[37] D. V. Senthilkumar, M. Lakshmanan, and J. Kurths, Phys. Rev. E **74**, 035205(R) (2006).
[38] G. V. Osipov, B. Hu, C. Zhou, M. V. Ivanchenko, and J. Kurths, Phys. Rev. Lett. **91**, 024101 (2003).
[39] N. Marwan, M. C. Romano, M. Thiel, and J. Kurths, Phys. Rep. **438**, 237 (2007).
[40] R. Q. Quiroga, J. Arnhold, and P. Grassberger, Phys. Rev. E **61**, 5142 (2000).
[41] M. Palus, V. Komarek, Z. Hrncir, and K. Sterbova, Phys. Rev. E **63**, 046211 (2001).
[42] A. Cenys, G. Lasiene, and K. Pyragas, Physica D **52**, 332 (1991).
[43] C. Zhou and J. Kurths, Phys. Rev. Lett. **88**, 230602 (2002).
[44] H. Lu and Z. He, IEEE Trans. Circuits Syst., I: Fundam. Theory Appl. **43**, 700 (1996).
[45] P. Thangavel, K. Murali, and M. Lakshmanan, Int. J. Bifurcation Chaos Appl. Sci. Eng. **8**, 2481 (1998).
[46] D. V. Senthilkumar and M. Lakshmanan, Int. J. Bifurcation Chaos Appl. Sci. Eng. **15**, 2895 (2005).
[47] J. D. Farmer, Physica D **4**, 366 (1982).
[48] D. V. Senthilkumar and M. Lakshmanan, Phys. Rev. E **71**, 016211 (2005).
[49] D. V. Senthilkumar and M. Lakshmanan, J. Phys.: Conf. Ser. **23**, 300 (2005).
[50] J. Kaplan and J. Yorke, *Functional Differential Equations and Approximation of Fixed Points*, edited by H. O. Peitgen and H. O. Walther (Springer, Berlin, 1979).
[51] M. C. Romano, M. Thiel, J. Kurths, I. Z. Kiss, and J. L. Hudson, Europhys. Lett. **71**, 466 (2005).
[52] H. D. I. Abarbanel, N. F. Rulkov, and M. M. Sushchik, Phys. Rev. E **53**, 4528 (1996).
[53] H. Kantz, and T. Schriber, *Nonlinear Time Series Analysis* (Cambridge University Press, New York, 1997).
[54] B. Hu, G. V. Osipov, H. L. Yang, and J. Kurths, Phys. Rev. E **67**, 066216 (2003).
[55] D. Gabor, J. IEE London **93**, 429 (1946).
[56] J. D. Farmer, Ann. N.Y. Acad. Sci. **357**, 453 (1980).
[57] E. F. Stone, Phys. Lett. A **163**, 367 (1992).